Robust Texture Features For Emphysema Classification In CT Images

Haipeng Li, Ramakrishnan Mukundan
Dept. of Computer Science and Software Engineering
University of Canterbury
Christchurch, New Zealand
0000-0001-7747-0180, 0000-0003-4578-1931

***Abstract*—In this paper, we propose a novel feature extraction method based on local quinary patterns (LQP), multifractal features and intensity histograms for classifying emphysema into three subtypes in computed tomography images. Compared to local binary patterns, LQP method computes more image local patterns to represent texture features. Multifractal features which enhancing local textures are combined with other features to constitute a feature vector for this classification task. An autoencoder network and principal components analysis are used to reduce the dimensionality of the feature vector before using an SVM classifier. The proposed method is tested on an emphysema database containing 168 annotated regions of interest of three different subtypes. The experimental results demonstrate that our method outperforms most other state-of-the-art approaches with the best classification accuracy of 92.3% using the least dimensionality (15) of the feature vector.**

Keywords—local quinary patterns, multifractal analysis, emphysema classification, autoencoder network

I. INTRODUCTION

Emphysema is one of the two main types of chronic obstructive pulmonary disease (COPD) which contains a group of progressive respiratory diseases that cause airflow blockage and breathing difficulties. Most people with COPD suffer from both emphysema and chronic bronchitis. Emphysema usually occurs when the air sacs of the lungs (alveoli) become damaged and enlarged, causing breathlessness [1]. More than 3 million people in the United States have been diagnosed with emphysema, and more than 11 million have COPD.

Pulmonary function tests (PFTs) can be used to diagnose emphysema, usually performing by spirometer. However, PFTs has low sensitivity and are not capable of detecting COPD at early stages. High resolution computed tomography (HRCT) imaging is another popular tool for diagnosing emphysema. CT imaging method is sensitive for diagnosing emphysema and is suitable to demonstrate the distribution and extent of emphysema patterns [2]. Emphysema in HRCT is characterised by the presence of areas of abnormally low attenuation which can be easily contrasted with surrounding normal lung parenchyma [3]. Webb et al. [4] classified emphysema into three subtypes: centrilobular emphysema (CLE), paraseptal emphysema (PSE) and panlobular emphysema (PLE).

The texture of lung tissue varies with different subtypes of emphysema; therefore, image texture analysis can be used to characterise the local image structure and classify emphysema in lung CT images [5]. Sørensen et al [6] proposed LBP based texture features to describe emphysema lesions and classified ROIs into three different types of emphysema. Their results reached high classification performance. Peng et al. [7] extended rotation invariant local binary pattern (RILBP) by considering Weber's law and used the combined features to classify emphysema into CLE and PSE. Multifractal features and LBP were cascaded in [8, 9] to capture more imaging features for lung tissue in CT images, including global spatial information. Other texture analysis technologies, such as gray-level co-occurrence matrices (GLCM) [10], discrete wavelet frame decomposition [11] and texton-based method [12], are proposed to extract texture features for the lung tissue classification.

The LBP method proposed by Ojala et al. [13] has been developed as a powerful descriptor for image classification and a reliable component in the texture analysis. It provides adequate knowledge about the local patterns with low computational complexity and is easy to combine with other feature vectors by using LBP histograms. For example, Sørensen et al. proposed to joint LBP and intensity histograms and form a 2D texture descriptor in their work [6]. In addition, LBP is extended to different variants for describing richer representation. Tan and Triggs [14] modified the approach by introducing Local Ternary Pattern (LTP) operators, which threshold the neighbouring pixels using a three-value encoding system based on a constant threshold set by the user. Nanni et al. [15] introduced a five-value encoding system called Local Quinary Pattern (LQP). The main difference is that the LBP, LTP and LQP threshold the neighbouring pixels into two (1 and 0), three (-1, 0 and 1) and five (2, 1, 0, -1 and -2) values, respectively. Although these formulations have achieved desirable performance, the curse of dimensionality is the major limitation [16]. High dimensionality of feature vectors not only causes extra computing cost but also affects the result performance (e.g. classification accuracy) due to partial redundant features.

This paper proposes a joint texture descriptor by using LQP, multifractal features and intensity histograms to classify pulmonary emphysema into three subtypes, namely, normal tissue (NT), CLE and PSE. LQP is considered, since it generates more texture patterns than LBP, which includes abundant imaging features can be used for this classification task. Multifractal analysis technology presents a strong property of enhancing image texture patters when applied in image classification [9, 17]. However, as introduced above, such multi-features concatenation will lead to high dimensionality for the extracted feature vector, which will negatively affect the following procedures in a classifier, increasing the complexity and weakening the classification sensitivity. Therefore, an autoencoder network and PCA method are employed subsequently to select important features and reduce the feature dimensionality to a lower level, which facilitates the classification. An SVM classifier uses the

extracted feature vector to produce the final classifying results. Fig. 1 shows a pipeline of the proposed method and more details are given in the following sections.

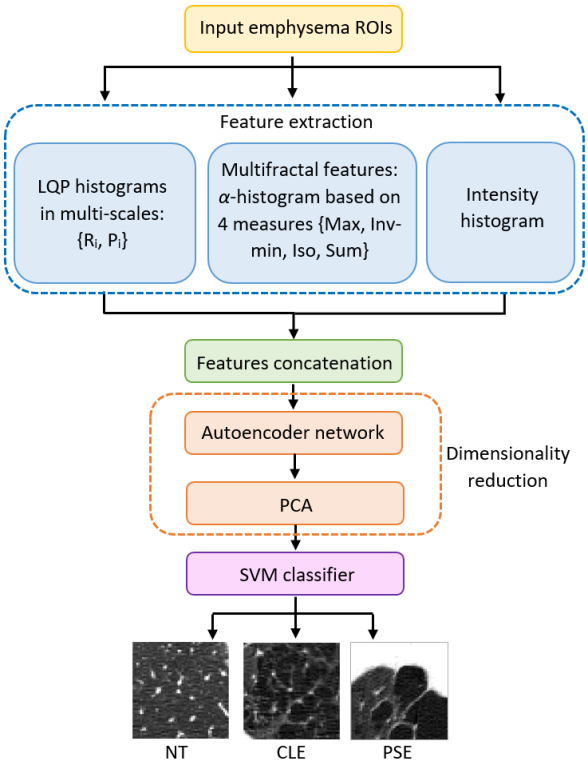

Fig. 1. The pipeline of the proposed method.

II. METHODS

A. Local quinary patterns (LQP)

In this study, LQP mathematical operators are used to extract local texture patterns, which is a variant of LBP. The conventional LBP code [13] of the pixel c is given by:

$$LBP(c,R,P) = \sum_{i=0}^{P-1} s(I_p - I_c)2^p \quad (1)$$

$$s(x) = \begin{cases} 1, & if\ x \geq 0 \\ 0, & if\ x < 0 \end{cases} \quad (2)$$

where R is the radius of the circle that form the neighbourhood, P is the number of pixels in the neighbourhood, I_c is the grey level value of the centre pixel c, and I_p is the grey level value of the pth neighbour.

Nanni et al. [15] modified the approach by introducing LQP operators, which threshold the neighbouring pixels using a five-value encoding system based on a constant threshold set $\{0, t_1, t_2\}$. The value of LQP code of the pixel c is given by:

$$LQP_i(c,R,P) = \sum_{p=0}^{P-1} s_i(I_p - I_c)2^p \qquad i = 1,2,3,4$$

$$s_1(x) = \begin{cases} 1, & x \geq t_2 \\ 0, & othetwise \end{cases}$$

$$s_2(x) = \begin{cases} 1, & t_1 \leq x < t_2 \\ 0, & othetwise \end{cases}$$

$$s_3(x) = \begin{cases} 1, & -t_2 \leq x < -t_1 \\ 0, & othetwise \end{cases}$$

$$s_4(x) = \begin{cases} 1, & x < -t_2 \\ 0, & othetwise \end{cases} \quad (3)$$

Once the LQP code is generated, it is split into four binary patterns as the $s_i(x)$ function indicated above. When P is set to be 8, each binary pattern, like an individual LBP, outputs its histogram with 256 bins; therefore, a high dimensional histogram (1024 bins) will be obtained using LQP, which contains more local texture features but also imposes some redundant information.

B. Multifractal analysis

Multifractal methods have been used to process and interpret medical images in some research work [9, 17], which demonstrate that it is an effective and promising tool for enhancing medical images and extracting texture features. There are four commonly used intensity measures in multifractal analysis: Maximum measure (Max), Inverse-minimum measure (Inv-min), Summation measure (Sum) and Iso measure (Iso). The function of a multifractal measure is denoted as $\mu_w(p)$, where p is the central pixel within a square window of size w. Let $g(k, l)$ represents the intensity value of the pixel at the position of (k, l) inside the window, and Ω denotes the set of all neighbourhood pixels of p in the window. Then the four measures can be formulated respectively as follows:

$$\text{Max:} \quad \mu_w(p) = \max_{(k,l\in\Omega)} g(k,l) \quad (4)$$

$$\text{Inv} - \text{min:} \quad \mu_w(p) = 1 - \min_{(k,l)\in\Omega} g(k,l) \quad (5)$$

$$\text{Sum:} \quad \mu_w(p) = \sum_{(k,l)\in\Omega} g(k,l) \quad (6)$$

$$\text{Iso:} \quad \mu_w(p) = \#\{(k,l)|g(p) \cong g(k,l), (k,l) \in \Omega\} \quad (7)$$

where, # is the number of pixels. In our experiments, pixel intensities in images are firstly normalized into the range of [0, 1] by dividing the maximum grey level value when considering Maximum and Inverse-minimum measures. Such normalization brings better image enhancing results due to the amplifying effect of the logarithmic function when computing the Hölder exponent in the domain of (0, 1).

The local singularity coefficient, also known as the Hölder exponent [18] or α-value, is used to depict the pointwise singularity of the object and its multifractal property quantitatively. Hölder exponent reflects the local behaviour of a function $\mu_w(p)$, which can be calculated by different intensity based measures mentioned above. The variation of the intensity measure with respect to w can be characterized as follows:

$$\mu_w(p) = Cw^{\alpha_p}, \quad w = 2i + 1, \ i = 0,1,2,\dots,d \quad (8)$$

$$log(\mu_w(p)) = \alpha_p\, log(w) + log(C) \quad (9)$$

where, C is an arbitrary constant and d is the total number of windows used in the computation of α_p. The value of α_p can be estimated from the slope of the linear regression line in a log-log plot where $\log(\mu_w(p))$ is plotted against $\log(w)$.

After computing the α value for each pixel in the processed image, α-images can be generated by using the α value to

replace the intensity value in the same position. All the α values in an α-image constitute a limited α value range [α_{min}, α_{max}]. This range can be equally divided into h sub-intervals and pixels with their α value locating in the same sub-interval would be counted for generating an α-histogram which will be used as feature histograms in this study.

C. Autoencoder network

Autoencoder networks are feed-forward neural networks with more than one hidden layer, attempting to reconstruct the input data at the output layer. The output layer is usually in the same size with the input layer and the network architecture represents a bell shape. As the size of the hidden layer in an autoencoder neural network is smaller, a high-dimensional input data can be reduced to narrower code space when using more hidden layers. Therefore, except image reconstruction and compression [19], autoencoder is also used to reduce feature dimensionality. Generally, an autoencoder network consists of two components namely "encoder" and "decoder". By reducing the hidden layer size, the encoder part is forced to learn important features of the input data and the decoder part reconstructs the original data from such feature code. Once the training phase is over decoder part is discarded and the encoder is used to transform a data sample to feature subspace.

In this study, we use autoencoder to reduce the length of feature histograms which concatenated LQP-histograms, α-histograms and intensity histograms. Therefore, a feature vector in shape of ($1\times n$) will be input into the autoencoder network for reducing its dimensionality (n). An autoencoder model containing 11 hidden layers is designed as illustrated in Fig. 2, in which input layer receives histogram features. Fully connected (FC) layers are used as hidden layers in this proposed structure and rectified linear unit (ReLU) is used as the activation function in each hidden layer except the last one layer which uses Sigmoid. Binary cross entropy is employed as a loss function.

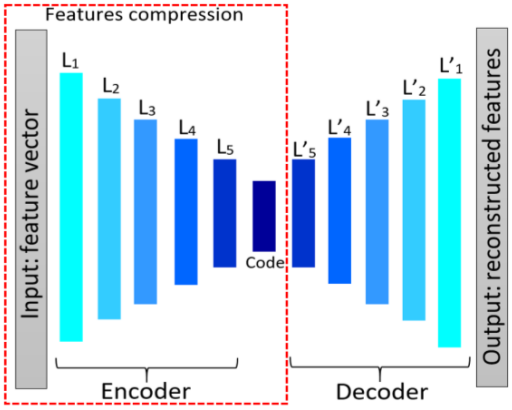

Fig. 2. The proposed autoencoder architecture for reducing feature numbers.

D. Principal components analysis (PCA)

PCA has been used in efficient coding of various biological signals [20]. It is a well-known optimal linear scheme for dimension reduction in data analysis. While retaining as much as possible the variance of the data set, PCA also contributes to improving algorithm performance and saving processing time.

In this study, X is used to denote the input feature vector which contains cascaded feature histograms. In order to obtain a new representation of the input data ($X=\{x_i,\ i=1,2,\ldots,N\}$), the covariance matrix $cov(X)$ is calculated as follows:

$$cov(X) = \frac{\sum_{i=1}^{N}(x_i-\bar{x})(x_i-\bar{x})^T}{N-1} \tag{10}$$

where n is the total number of features in X and $\bar{x}$ is the mean of X. Then the eigenvalues and eigenvectors of the matrix $cov(X)$ are calculated and the eigenvectors will be sorted in descending order according to the eigenvalues. The reduced feature vector (X') can be derived from X and eigenvectors matrix V as follows:

$$X' = X \cdot V \tag{11}$$

In PCA, an assumption made for feature selection is that most information of the input vectors is contained in the subspace spanned by the first n principal axes, where $n < N$ for a N-dimensional feature space. Therefore, each original feature vector can be represented by its principal component vector with dimensionality of n.

E. Classifier

SVM is used in our experiments to produce the final classification results. One key point when using SVM classifier is to find a proper kernel and the optimum parameters (*gamma* and C). A radial basis function (RBF) kernel is selected as it is used and recommended in [12, 21] as the first choice. The parameters of *gamma* (kernel width) and C are found using a grid search procedure on the training set. In addition, leave-one-subject-out policy [6] is imported in the grid search, which means every time ROIs from one patient are removed as the test set and the remaining parts as the training set.

III. Experiments and Results

A. Dataset

The CT Emphysema dataset used in our experiments is the Bruijne and Sørensen database [6] which is available for the academic research from their homepage. It consists of 168 non-overlapping annotated ROIs of size 61 × 61 pixel patches from three different classes: NT (59 patches), CLE (50 patches), and PSE (59 patches). Examples of each class are showed in Fig. 1. This ROI set comes from 25 subjects (patients). In experiments, leave-one-subject-out method is used to evaluate classification performance.

B. Parameter selection and feature extraction

As introduced in section 2, this study mainly consider LQP, multifractal features and intensity histograms for feature extraction and autoencoder and PCA are used to reduce feature dimensionality. For LQP operators, in order to include more local texture information from neighbourhood, different $\{R_i, P_i\}$ pairs are tested and cascaded to construct multi-scales feature vectors. Parameters of t_1 and t_2 in LQP are set to be 5 and 12 respectively which keeps the same settings in [22]. In multifractal analysis, h=100 is designated to divide α value range [α_{min}, α_{max}] into h sub-intervals and generate its α-histograms.

The following five extracted feature vectors are evaluated and compared:

1) LQP1: LQP histograms with $\{R_1=1, P_1=5\}$.

2) LQP2: LQP histograms in two scales with $\{R_1=1, P_1=5\}$ and $\{R_2=2, P_2=8\}$ are connected.

3) LQPIN: Joint LQP2 and intensity histograms.

4) LQPIA1: LQP1, intensity histograms and alpha histograms (4 measures) are cascaded.

5) LQPIA2: LQP2, intensity histograms and alpha histograms (4 measures) are cascaded.

Multi-scales LQP produces feature histograms with high dimensionality, for example, LAPIA2 generates the longest feature histogram (1808 bins) among the five approaches, which is too heavy for a classifier and cannot present effective classifying results. Here, autoencoder network introduced in section 2 is used to reduce the feature dimensionality (n) to a specific size s (code layer size). Different s (16, 32, 64, 128, 256) has been tested, finally s=64 is used with better performance. This model is trained using the stochastic gradient descent (SGD) method with batch size of 128 for 300 epochs. Other parameters are optimized using the adaptive moment estimation (Adam) method to minimize the binary entropy loss. PCA procedure follows the autoencoder to further reduce the length of the feature vector.

The final dimensionality-reduced feature vector (n<64) is input to an SVM classifier for classifying the emphysema ROIs into three subtypes. The SVM classifier with RBF kernel finds the optimum parameters of gamma and C in range of $[10^{-2}, 10^{10}]$ and $[10^{-9}, 10^{3}]$ respectively using a grid search. Fig. 3 shows that for LQPIA2 with the reduced features (n=15), the best parameters are C=10 and $gamma$=0.01 with a classification accuracy of 0.92.

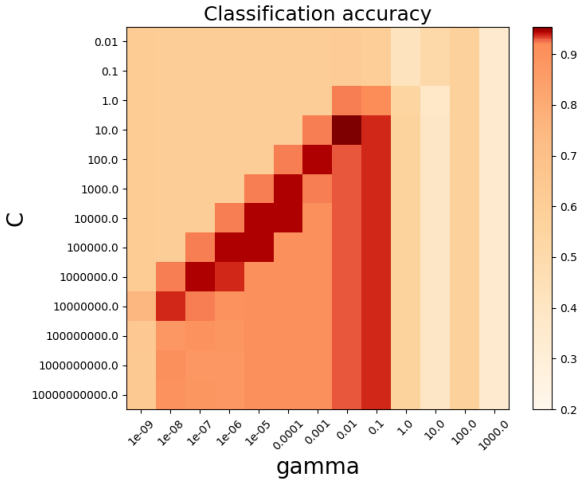

Fig. 3. The heatmap of the classificaiton accuracy in a grid search.

C. Feature dimensionality reduction

In this study, autoencoder network and PCA technology are used to select and reduce the extracted feature histograms with the aim of producing the optimum n-dimensional feature vector used for classification. Different hidden layers in autoencoder structure are tested in range of [5, 15] and an 11-layer architecture (as showed in Fig. 2) with the code layer size s=64 is used in experiments. Four out of the five feature extraction approaches listed above use autoencoder to reduce the dimensionality (n) of feature vectors (LQP1 with 128 features directly uses PCA). When using autoencoder network, neuron numbers in each hidden layer is set to decreased averagely from its input layer to the core code layer (s=64) for the encoder part and decoder part uses the inverse operations. In our experiments, when s is set to be lower than 64 (e.g. 16 or 32), the final corresponding classification accuracy falls to lower levels. The experimental results indicate that the proposed autoencoder network can reduce feature dimensionality effectively by compressing redundant information and remaining important parts with a proper code layer size (s). When s is too small, some important features begin losing as well. While PCA method based on the 64-length feature vector is performed to re-compute it and output new features in decreasing order which can be used to select the best and shortest top n dimensional features. Fig. 4 shows the changes of classification accuracy when n is reduced from 64 to 1 using five different approaches.

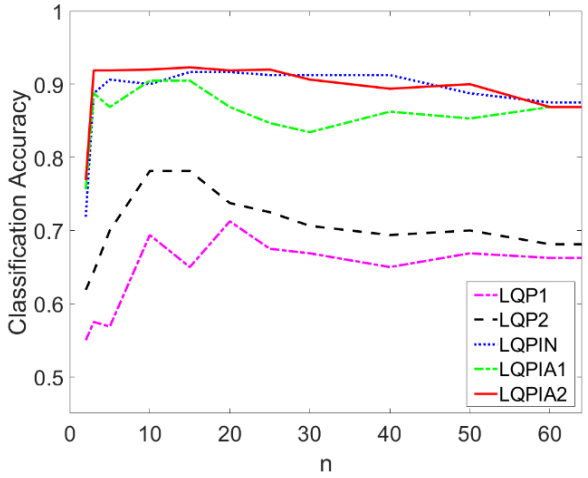

Fig. 4. The comparison among different approaches using the reduced feature numbers (n) to classify emphysema ROIs into three types.

D. Results comparision and discussion

In this study, we concentrate on classifying three subtypes of emphysema. Different methods tested on the same database are compared in Table 1. Specifically, rotation invariant Gaussian filter bank (GFB1), rotation invariant LBP (LBP1) and joint 2D LBP and intensity histograms (LBP2) are approaches reported in [6]. MFS refers to multifractal spectrum method used in [9]. From Table 1, we can see that the classification performance using our proposed method (LQPIA2) reached 92.3% (Table 2) which is close to the best result in [6, 12]. Meanwhile, the dimensionality of the feature vector used in our method is 15 which is much lower than that in the LBP2 method. In addition, when comparing with other methods using fewer features, such like GFB1 used 16 features, our methods present much higher classification performance.

Moreover, some reported methods focus on two subtypes classification (CLE vs. PSE). In Table 3, JINT1 and JINT2 are methods reported in [7] using refined rotation invariant local ternary patterns combined intensity histograms. MFA is a method uses alpha histograms based on multifractal analysis [9]. While our proposed method (LQPIA2) represents the best classification accuracy by using only 5 features for this two categories classification.

TABLE I. METHODS COMPARISON FOR THREE SUBTYPES CLASSIFICATION.

Methods	Dimension	Classification Accuracy (%)
GFB1[6]	16	61.3
LBP1[6]	36	79.2
LBP2[6]	324	95.2
Texton-based[12]	120	96.4
MFS[9]	200	69.0
LQP1	20	71.3
LQP2	10	78.1
LQPIN	15	91.7
LQPIA1	15	90.5
LQPIA2	15	92.3

TABLE II. CONFUSION MATRIX WITH BEST CLASSIFYING RESULT USING LQPIA2 METHOD.

		Predicted		
		NT	CLE	PSE
Actual	NT	53	4	2
	CLE	1	48	1
	PSE	5	0	54

TABLE III. METHODS COMPARISON FOR TWO SUBTYPES CLASSIFICATION.

Methods	Dimension	Classification Accuracy (%)
JINT1[7]	180	95.2
JINT2[7]	900	95.8
LBP2[6][7]	324	92.2
Texton-based[7][12]	120	90.5
MFA[9]	100	92.0
LQPIA2	5	98.8

IV. CONCLUSION

This paper proposes a novel texture feature extraction method based on local quinary pattern (LQP) operators, multifractal features and intensity histograms, with the aim of classifying emphysema into three subtypes in CT images. In order to adequately capture local texture information, LQP based feature histograms are obtained in different local region scales and are concatenated with other imaging features to form a high-dimensional feature vector. For removing redundant features and remaining important parts in the feature vector, an autoencoder network is designed to reduce the feature dimensionality, which is followed by a PCA procedure for selecting the best top *n* features. An SVM classifier with a RBF kernel is used in this study to produce the classification results. Using the dimensionality-reduced feature vector, the classifying process can be done effectively and efficiently. Comparing with the state-of-the-art methods, the length of the feature vector used in our proposed method is reduced by more than 95% (324 vs. 15) and the result accuracy is observed in a similar level (0.95 vs. 0.92).

REFERENCES

[1] Fiel B. (1996). Chronic obstructive pulmonary disease. Drugs52(2):55–61.

[2] Chabat DHF, Yang G. (2003). Obstructive lung diseases: texture classification for differentiation at CT Radiology. 228(3): 871–877.

[3] Sørensen L, de Bruijne M. (2009). Dissimilarity representations in lungparenchyma classification. In Proceeding of the Spie digital library Conference, Medical imaging; Computer-Aided Diagnosis. 7260(27) : 1–12.

[4] W. R. Webb, N. Müller, and D. Naidich. (2001). High-Resolution CT of the Lung, Third Edition, J.-R. John, Ed. Lippincott Williams & Wilkins.

[5] A. H. Mir, M. Hanmandlu, and S. N. Tandon. (1995). Texture analysis of CT images. IEEE Eng. Med. Biol. Mag, 14(6): 781–786.

[6] Sørensen, L., Shaker, S. B., & de Bruijne, M. (2010). Quantitative Analysis of Pulmonary Emphysema Using Local Binary Patterns. IEEE Transactions on Medical Imaging, 29(2), 559-569. doi:10.1109/Tmi.2009.2038575

[7] Peng, L., Lin, L., Hu, H., Ling, X., Wang, D., Han, X., & Chen, Y. (2017). Joint weber-based rotation invariant uniform local ternary pattern for classification of pulmonary emphysema in CT images. Paper presented at the 2017 IEEE International Conference on Image Processing (ICIP).

[8] Ibrahim, M. A., & Mukundan, R. (2015). Analysis of Scale Variations of Local Features for Accurate Classification of Emphysema Images. 2015 8th International Conference on Biomedical Engineering and Informatics (BMEI), 6-13.

[9] Ibrahim, M., & Mukundan, R. (2015). Cascaded Techniques for Improving Emphysema Classification in CT Images. Artificial Intelligence Research, 4(2), 112-118. https://doi.org/Doi:10.5430/air.v4n2p112

[10] Sluimer, I.C., Prokop, M., Hartmann, I., van Ginneken, B. (2006). Automated Classification of Hyperlucency, Fibrosis, Ground Glass, Solid, and Focal Lesions in High-Resolution CT of the Lung. Medical Physics 33(7), 2610–2620.

[11] A. Depeursinge, D. Sage, A. Hidki, A. Platon, P.-A. Poletti, M. Unser, and H. Muller. (2007). Lung tissue classification using wavelet frames. In Proc. 29th Annual International Conference of the IEEE Engineering in Medicine and Biology Society EMBS 2007, 6259–6262.

[12] M. J. Gangeh, L. Sørensen, S. B. Shaker, M. S. Kamel, M. de Bruijne, and M. Loog. (2010). A texton-based approach for the classification of lung parenchyma in CT images, Medical Image Computing and Computer Assisted Intervention (MICCAI).

[13] Ojala, T., Pietikäinen, M., & Harwood, D. (1996). A comparative study of texture measures with classification based on featured distributions. Pattern Recognition, 29(1), 51-59. doi:https://doi.org/10.1016/0031-3203(95)00067-4

[14] Tan, X., & Triggs, B. (2007). Enhanced local texture feature sets for face recognition under difficult lighting conditions. In Analysis and Modelling of Faces and Gestures; Springer: Berlin/Heidelberg, Germany, 168–182.

[15] Nanni, L., Luminia, A., & Brahnam, S. (2010). Local binary patterns variants as texture descriptors for medical image analysis. Artif. Intell. Med, 49, 117–125.

[16] Yelampalli, P.K.R., Nayak, J. & Gaidhane, V.H. (2019). A novel binary feature descriptor to discriminate normal and abnormal chest CT images using dissimilarity measures. Pattern Anal Applic 22, 1517–1526. https://doi.org/10.1007/s10044-018-00771-2

[17] Li H., Mukundan R., Boyd S. (2020). A Novel Application of Multifractal Features for Detection of Microcalcifications in Digital Mammograms. In: Zheng Y., Williams B., Chen K. (eds) Medical Image Understanding and Analysis. MIUA 2019. Communications in Computer and Information Science, vol 1065. Springer, Cham.

[18] Falconer K. (2005). Random Fractals. Fractal Geometry: Mathematical Foundations and Applications, Second ed Chichester. UK: John Wiley & Sons.

[19] Bai, J., Dai, X., Wu, Q., & Xie, L. (2018). Limited-view CT Reconstruction Based on Autoencoder-like Generative Adversarial Networks with Joint Loss. Paper presented at the 2018 40th Annual International Conference of the IEEE Engineering in Medicine and Biology Society (EMBC).

[20] Hyvarinen, A., Karhunen, J. & Oja, E. (2001). Independent Component Analysis. New York: J Wiley.

[21] Fan, R.E., Chen, P.H., Lin, C.J. (2005). Working Set Selection Using the Second Order Information for Training SVM. Journal of Mach. Learning Research 6, 1889–1918.

[22] Rampun, A., Scotney, B. W., Morrow, P. J., Wang, H., & Winder, J. (2018). Breast Density Classification Using Local Quinary Patterns with Various Neighbourhood Topologies. Journal of Imaging, 4(1). https://doi.org/UNSP 1410.3390/jimaging4010014